

A Visual Servo System for Microinjection under Stereoscopic Microscope

Hideki Yamamoto Tetsuya Sano

Junko Sakiyama Motoi Okamoto

Faculty of Education Okayama University
Tsushima 3-1-1, Okayama, 700-8530, Japan
yamamoto@cc.okayama-u.ac.jp

Faculty of Health Sciences,
Okayama University Medical School.
Okayama, Okayama, 700-8558, Japan
Email: sakisaki@md.okayama-u.ac.jp

Abstract

In this paper, we describe a visual feedback system that controls a micromanipulator so that a needle may pierce a target as much length as desired under a stereoscopic microscope. At first, we proposed a strategy of moving the needle head for achieving the microinjection procedure at a realistic rate. Secondly, we developed a prediction method of the needle head within the target. Before the needle pierces the target, the shape of the needle head is preserved as a reference pattern. After the needle piercing the target, the shape of the needle head within the target is predicted using the reference pattern and the tip position of the needle head can be detected. Experimental results indicate that the proposed system may be useful in micromanipulation such as microinjection to a slice of rat brain.

sufficiently with the cells in various thickness because the manipulator of the AIS moves constantly regardless of the distance between the injector and the cells. An automatic microinjection system that controls the injector that may pierce cells in the desired depth is needed for achieving the injection procedure.

In this paper, an automatic microinjection system under the stereoscopic microscope by using well-known techniques of visual feedback is realized. Lately, the several techniques of visual feedback are proposed[5, 6]. However, these systems have some problems in performing the microinjection. The first problem is to estimate parameters for the measurement of distance under the stereoscopic microscope. The second problem is to detect the tip of the needle head after piercing the target, and to decide whether the needle head pierces the target in the desired depth.

Therefore, in this system, the measurement of the distance under the stereoscopic microscope is automatically carried out by image processing. In order to control the depth of the needle head within the target, a prediction method, which determines the tip position of the needle head within the target, is developed. Experimental results indicate that the proposed system may be useful in microinjection.

1. Introduction

In the area of biotechnology, microinjection system is widely used for such purposes as operating on genes and transferring biological materials into cells. For the some experiments, such as biochemical assay, a large number of cells have to be injected in a short time. The development of a computer-assisted and microprocessor-controlled injection system provides high injection rates. The AIS(automated injection system, Zeiss, Germany) is an automated microinjection system, and it permits reliable and simple microinjection into living cells by a system configuration of various hardware and software components that controls the injection procedure [1].

The AIS cannot perform the injection procedure

2. Methods

Figure 1 shows the microinjection system. The system consists of a stereoscopic microscope, two CCD cameras, a micromanipulator, and a personal computer. A slice of rat brain is set on the stage of the microscope. The cameras are mounted to the eyepieces of the microscope. The micromanipulator has three degrees of freedom. It moves linearly. The needle is set to the micromanipulator. The

left image and the right image are inputted to the personal computer. The distance between the needle head and the target is measured three dimensionally by the stereovision method. The needle head is guided to reduce the distance between the tip position of the needle head and the goal to 0.

A template image of the target and color information of the target are obtained for detecting the target that is unclear in the image before starting the microinjection procedure. The template image is the binary image of the target. The color information is the thresholding values estimated by the average value and the standard deviation of the gray levels of the target in the image. The color images of the CCDs are converted into gray level images. The noise reduction is performed by a median filtering. The pixels that are near to the target in gray level are detected by thresholding. The target is detected from the images by the method of template matching[4].

The gray levels of the needle head are greatly different from the gray levels of the other areas in the image. The needle head is detected by the thresholding. The average of gray levels is estimated as the thresholding values.

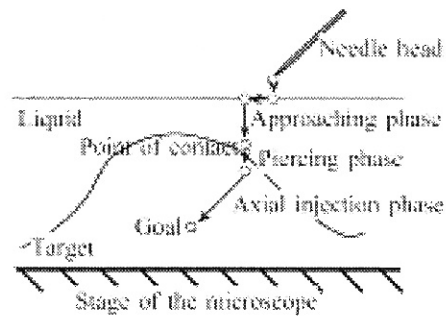
Figure 2 shows the path of the needle head. At first, the needle head approaches to a point of contact that is set on the surface of the target where the needle head begins to pierce the target as shown in figure 2 b). The needle head is descending vertically until it touches the liquid surface. Then the needle head is guided to the point of contact three dimensionally. In this phase, the distance between the needle head and the point of contact is measured three dimensionally by the stereovision method. Secondly, the needle head is guided to pierces the surface of the target to avoid the needle head slipping the target. In piercing phase, the needle head descends gradually on the point of contact. The needle head distorts the surface of the target.



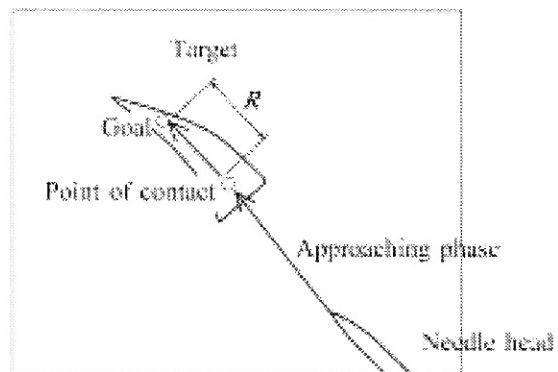
Fig. 1 Microinjection system.

The condition of the injection is checked at constant interval. Finally, the axial injection is performed until the needle head reaches the goal. The needle head gradually proceeds within the target during the axial injection phase. The tip position of the needle head is detected by pattern matching.

Figure 3 shows the needle head before piercing and the needle head after piercing. Before the needle head pierces the target, shape of the needle head is sharp as shown in figure 3 a). After the needle head piercing the target, the surface of the rat brain is restored, and a part of the tip of the needle head is hidden. The tip of the needle head becomes round shape as shown in the figure 3 b). In order to evaluate the sharpness of the needle head, the size of the tip area is measured as shown in figure 4. The tip size is larger in the round shape than the tip size in the sharp shape. The tip size of the needle head indicates whether the needle head pierces the target or not. The size of the tip area is almost constant during the approaching phase. In this phase, the average and the standard deviation of the tip area is derived. In piercing phase, the size of the tip area increases constantly. It considers that the needle head pierces the target when the area becomes bigger than the



a) XY plane



b) XZ plane

Fig. 2 Path of the needle head.

sum with the average and the standard deviation of the tip area. Finally, the needle head proceeds to the goal within the target. The tip position of the needle head is detected by an algorithm as follows.

Figure 5 shows a schematic of the needle head after piercing. A square region of interest is set automatically after the needle head is detected. The tip position of the needle head is on a diagonal line of the square region. The binary image of the needle head in the region is preserved as the reference pattern. When the needle pierces the target to the depth desired, the tip part of the needle becomes invisible. The reference pattern is divided into two areas. When the needle pierces the target, the tip part of the needle becomes invisible. This area is named as an invisible area. The remaining part is named as a visible area. The visible area indicates the shape of the needle head after the needle head reaches the goal. The visible area is used to detect the position of the reference pattern in the image after the needle head pierces the target. The invisible area is used to predict the tip position of the needle head. The length R is estimated from the length of the needle head piercing as shown in figure 6.

When the needle head pierces the target, the part of the

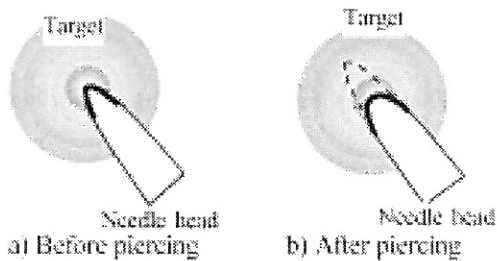


Fig. 3 Shape of the needle head.

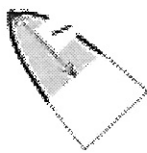


Fig. 4 Size of the tip area.

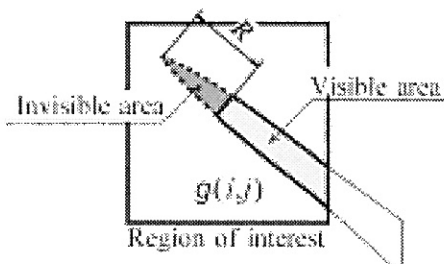


Fig. 5 Reference pattern.

needle head corresponding to the visible part of the reference pattern is searched as shown in Figure 7. Because the tip of the needle is on the center line of the needle head. At first, the centerline of the needle head is estimated. Secondly, in order to perform the template matching, regions of interest $f_k(i, j)$ ($k=1, 2, \dots, n$) are set on the centerline. Each region's upper left corner is on the centerline. One of the regions will indicate the position of the reference pattern. The region of interest $f_k(i, j)$, where the correlation r_k is closest to 1.0, indicates the position of the reference pattern. The shape of the needle head in the invisible part can be predicted by using the invisible area of the reference pattern.

3. Experimental results

A microinjection with a stereoscopic microscope having a magnification of 10 times is performed. A steel needle is attached to a micromanipulator. Figure 8 shows the relation, which is the position difference of the needle head and the distance between the tip position and the object lens of the microscope. The measurement resolutions are as shown in Table 1.

Figure 9 shows an example of the prediction of the needle head. The image indicates the needle head piercing the target at desired length. Figure 10 shows the values of correlation between the reference pattern and the needle

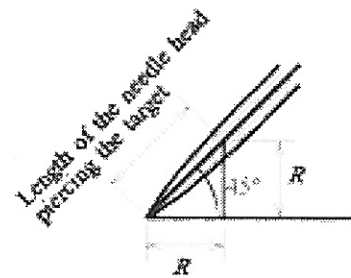


Fig. 6 Length of the needle head piercing the target.

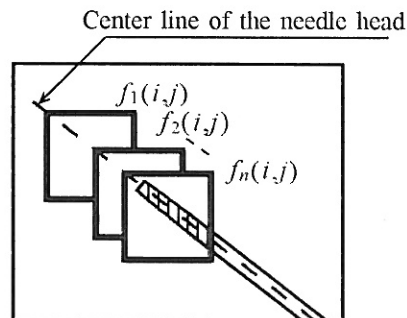


Fig. 7 Search method of the tip position of the needle head within the target.

head. The horizontal axis represents positions of the reference pattern. A position where the correlation value becomes maximum value indicates the position of the reference pattern. The needle head is predicted that it pierces the target 0.44mm in length as shown in figure 9.

Next, the proposed system is applied for the microinjection into a rat brain. A glass microelectrode is filled with lipophilic fluorescent tracer DiI or DiD and the microelectrode is connected to a microinjector with a Teflon tube. A coronal slice of adult Sprague-Dawley rat brain of (5mm in thickness) was placed in a recording chamber filled with phosphate-buffered saline as shown in figure 11. The mean concentration was 92.93 and the standard deviation was 5.39 respectively.

At first, a template image was made from microscopic photos of cresyl violet-stained coronal section of the rat brain that is shown in figure 12. A clearly defined image of the dentate gyrus was obtained by this processing because the granule cells were strongly stained with cresyl violet compared to adjacent molecular layer and hilar region. The template of the apex of the dentate gyrus is obtained as shown in figure 13. The position of the template in the image is sequentially scanned in parallel translation and the common region between the template and the image is compared for similarity. We estimated the correlation between the template and the image for the comparison of the similarity. The location of the template where the correlation became maximum value was detected. Then, the template was scanned over the image in rotation translation. As the same method, the angle of the apex was

detected as shown in Fig. 14. The triangular-shaped apex of granule cell layer was clearly visualized. The maximum correlation coefficient was 0.330375 when the center of the template image was located at $i=174$ $j=311$ in the image.

The shape of the lipophilic fluorescent tracer in the microelectrode is derived as the reference pattern. However, the length of the reference pattern is shorter than the desired length of the microelectrode piercing the target. Therefore, the speed of the micromanipulator in the axial injection is derived during until the tracer can be seen in the image. The rest of the distance is predicted when the tracer becomes invisible. The microelectrode is guided to the goal blindly. The tip of microelectrode was successfully inserted into the target region and DiI or DiD

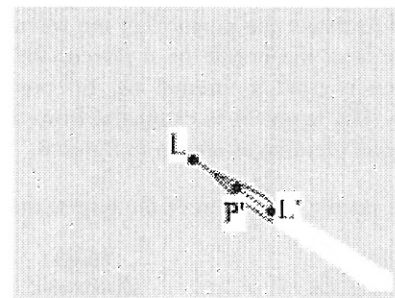


Fig. 9 Example of the prediction of the needle head.

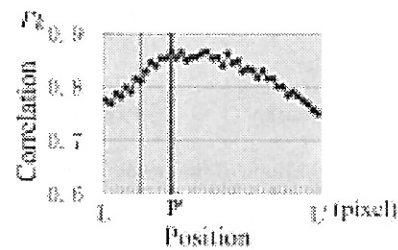


Fig. 10 Correlation values between the reference pattern and the image.

Table 1. Resolutions of the image measurement.

X	0.0096mm/pixel
Y	0.0366mm/pixel
Z	0.0095mm/pixel

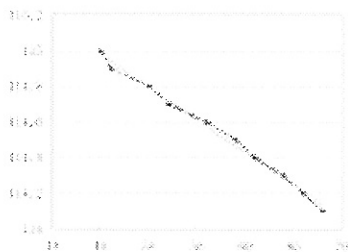


Fig. 8 The position difference of the tip position of the needle head and the distance between the tip position and the object lens.



Fig. 11 Dentate gyrus of rat brain.

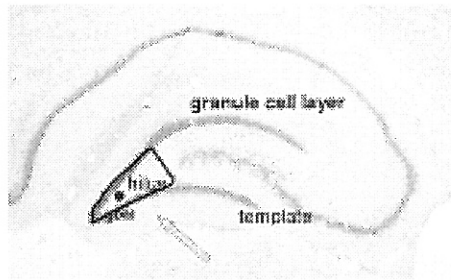


Fig. 12 Cresyl violet-stained coronal section of the rat brain.



Fig. 13 Template of the apex of the dentate gyrus.

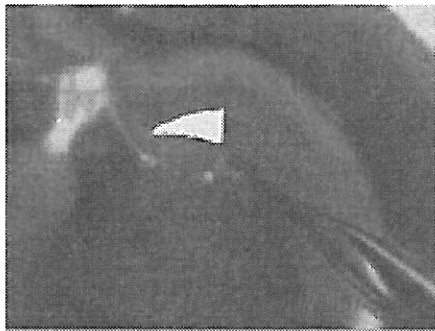


Fig. 14 Detected triangular-shaped apex of the dentate gyrus where lipophilic tracers are to be injected.



Fig. 15 Needle head piercing the target

was slowly injected by a nanotransjector as shown in figure 15. Figure 16 shows the microelectrode pulling out of the rat brain.

□□ In the present study, we injected lipophilic tracer into 4% paraformaldehyde-fixed brain slices because lipophilic

tracers were incorporated into plasma membrane are slowly dispersed along the outer layer of plasma membrane and provide sharp morphological image. Moreover, lipophilic tracers can be injected into 5 mm brain slice was processed as described in the methods. By using an automated micromanipulation device, the tip of microelectrode was successfully inserted into the apex of dentate gyrus by 6 to 8 steps of movements within 2 to 3 minutes, and 0.5 to 1 μ l of lipophilic tracer was injected into granule cell layer.

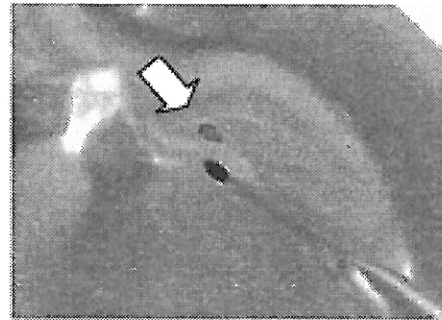


Fig. 16 Coronal slice injected lipophilic tracer into the apex of the dentate gyrus. The injected site is indicated by arrow.

4. Conclusions

In this paper, an automatic microinjection system for use with a stereoscopic microscope that includes visual feedback is proposed. A strategy of moving the needle head for achieving the microinjection procedure at a realistic rate is proposed. A prediction method of the needle head within the target is developed. During the needle proceeds within the target, the tip position of the needle head is predicted by the correlation matching. As a result, the tip position of the needle head within the target is fully estimated and effectively guided to reach a goal within the target.

We have shown that our visual image processing and automated micromanipulation could be utilized for lipophilic tracer injection into the hilus of the dentate gyrus of rat brain slice. Local injection of tracers has been done by microscopic visual inspection and control of microelectrode.

5. REFERENCES

- [1] W. Ansorge and R. Saferich. Microinjection and Transgenesis Strategies and Protocols. Springer Lab Manual, pages 31-46, 1998.

- [2] J. Liu and Y. Yang. Multiresolution color image segmentation. *IEEE Transactions on Pattern Analysis and Machine Intelligence*, 16(7):689-700, 1994.
- [3] T. Sano H. Nagahata and H. Yamamoto. Automatic Micromanipulation System Using Stereoscopic Microscope. *IMTC '99*, 1:327-331, 1999.
- [4] T. Sano and H. Yamamoto. Micromanipulation using Stereoscopic Microscope. *ISIE'99 Proceedings of the IEEE International Symposium on Industrial Electronics*, 3:1066-1069, 1999.
- [5] J.T. Feddeman and G.C.S. Lee and O.R. Mitchell. Model-based Visual Feedback Control for Hand-Eye Coordinated Robotic System. *IEEE Computer*, pages 21-31, 1992.
- [6] A. Castano and S. Hutchinson. Visual compliance: Task-directed visual servo control. *IEEE Transactions ON ROBOTICS AND AUTOMATION*, 10(3):334-341, 1994.
- [7] T.L. Babb, W.J. Brown, J. Pretorius, C. Davenport, J. Lieb and P.H. Crandall, "Temporal lobe volumetric cell densities in temporal lobe epilepsy", *Epilepsia*, Vol.25, pp.729-740, 1984
- [8] R.S. Sloviter, "The functional organization of the hippocampal dentate gyrus and its relevance to the pathogenesis of temporal lobe epilepsy", *Ann Neurol*. Vol.35, pp.640-654, 1994
- [9] C.R. Houser and M. Esclapez, "Vulnerability and plasticity of the GABA system in the pilocarpine model of spontaneous recurrent seizures", *Epilepsy Res*. Vol.26, pp.207-218, 1996
- [10] P.S. Buckmaster and A.L. Jongen-Relo, "Highly specific neuron loss preserves lateral inhibitory circuits in the dentate gyrus of kainate-induced epileptic rats", *J. Neurosci.*, Vol.19, pp.9519-9529, 1999
- [11] E. Soriano and M. Frotscher, "Mossy cells of the rat fascia dentate are glutamate-immunoreactive", *Hippocampus*, Vol.4, pp.65-69, 1994
- [12] T. Fukuda and T. Kosaka, "Gap junctions linking the dendritic network of GABAergic interneurons in the hippocampus", *J. Neurosci.*, Vol.20, pp.1519-1528, 2000
- [13] M.G. Honig and R.I. Hume, "Fluorescent carbocyanine dyes allow living neurons of identified origin to be studied in long-term cultures", *J. Cell Biol.*, Vol.103, pp.171-187, 1986
- [14] R. Linke and M. Frotscher, "Development of the rat septohippocampal projection: tracing with Dil and electron microscopy of identified growth cones", *J. Comp. Neurol.*, Vol.332, pp. 69-88, 1993
- [15] D.G. Amaral and M.P. Witter, "The three-dimensional organization of the hippocampal formation: a review of anatomical data", *Neuroscience*, Vol.31, pp.571-591, 1989
- [16] H. Yamamoto and T. Sano, "Visual feedback system for micromanipulation" *WISP'99*, Budapest, Hungary, pp.353-358, 1999